



Predicting Blast-Induced Ground Vibrations in Some Indian Tunnels: a Comparison of Decision Tree, Artificial Neural Network and Multivariate Regression Methods

Aditya Rana¹ · N. K. Bhagat¹ · G. P. Jadaun¹ · Saurav Rukhaiyar¹ · Anindya Pain² · P. K. Singh¹

Received: 14 August 2019 / Accepted: 13 March 2020
© Society for Mining, Metallurgy & Exploration Inc. 2020

Abstract

The present study compares three different techniques (decision tree, artificial neural network and multivariate regression analysis) for predicting blast-induced ground vibrations in some Indian tunnelling projects. The performance of these models was also compared to site-specific conventional predictor equations. A database consisting of 137 vibration records was randomly divided into training and testing sets for model generation. Eight input parameters (total charge, tunnel cross-section, maximum charge per delay, number of holes, hole diameter, distance from blasting face, hole depth and charge per hole) were selected for model development using bivariate correlation analysis. Results indicated that the decision tree is best suited for predicting vibrations. The decision tree further suggested that the intensity of near-field ground vibrations is mainly affected by total charge fired in a round, whereas the intensity of far-field vibrations is governed by maximum charge per delay and charge per hole. Conventional ground vibration predictors and machine learning techniques such as neural networks do not depict the relationship between input and output parameters. However, the present study substantiates that the decision tree can be a good tool for precise prediction of ground vibrations. Further, the decision tree can classify and relate different blast design parameters for refining blast designs to control ground vibrations on sites.

Keywords Decision tree · Artificial neural network · Blasting · Ground vibration · Tunnelling

Abbreviations

ANN	Artificial neural network
CART	Classification and regression tree
MCPD	Maximum charge per delay
MVRA	Multivariate regression analysis
PPV	Peak particle velocity
RMSE	Root mean square error

1 Introduction

The drill and blast method is the most widely used technique for rock excavation in tunnelling and underground projects. Its

suitability for medium to hard ground conditions has been well recorded [1]. The drill and blast method is not only economical in comparison to mechanical methods like tunnel boring machine, road header, etc., but it can also be used to obtain varying tunnel profiles. Past researches indicate that only 20–30% of explosives are utilised for rock fragmentation and the remaining 70–80% yield unwanted effects such as ground vibrations, fly-rock, noise, etc. in surface mining [2, 3]. The ground vibrations from uncontrolled rock blasting pose an adverse impact on surrounding rock mass, natural habitats, buildings and structures. The engineering structures are highly prone to damages caused by blast vibrations associated with low frequencies between 4 and 24 Hz (Directorate General of Mines Safety 1997). This is because the frequency of ground vibrations resonates with the natural frequency of structures causing more damage. It is often observed that the people living nearby these projects erroneously co-relate damages in their households with the blast vibrations. This results in protest, confrontation, delay and occasional closure of the projects. Intense blast vibrations produced by uncontrolled blasting may also damage the available groundwater channels and harm the surrounding ecology. These vibrations can be

✉ Aditya Rana
adityarana@cimfr.nic.in

¹ CSIR-Central Institute of Mining and Fuel Research, Dhanbad, Jharkhand, India

² CSIR-Central Building Research Institute, Roorkee, Uttarakhand, India

effectively controlled by varying blast design parameters. Hence, the prediction of blast-induced vibrations and assessment of their effects are generally done before the commencement of blasting activities.

Peak particle velocity (PPV) is the most preferred predictor to evaluate blast-induced ground vibration. Almost all the predictor equations estimate PPV considering only two parameters, i.e. maximum charge per delay (MCPD) and distance between blast face to monitoring points. Some predictor equations also consider attenuation or damping factors for the prediction of PPV. It has been observed that the prediction of these equations is inconsistent [4]. These predictor equations have their limitations which affect the prediction of the vibrations. PPV is observed to be influenced by various other parameters such as geological and geotechnical conditions, blast geometry, the total explosive used, etc. The empirical predictor equations do not consider these and hence have low accuracy. For tunnelling and underground projects, these parameters play a significant role. Recently, researchers have effectively demonstrated the use of advance statistical and soft computing tools for the prediction of ground vibrations considering the aforementioned parameters. Soft computing techniques such as genetic programming, maximum likelihood classification, technique for order preference similarity to ideal solutions, support vector machine, artificial neural network (ANN) and classification and regression tree (CART) have been effectively used for predicting blast vibrations and other blast design parameters. Decision tree-based learning methods such as CART split or classify data (at nodes) into smaller datasets and generate small linear models using regression. These linear models together generalise the final model for minimising RMSE (root mean square error) at each node. These models are easy to comprehend unlike neural networks and machine learning tools. The applicability of decision tree or CART in predicting PPV has not been extensively studied. Hasanipanah et al. [5] forecasted blast-induced ground vibrations for Miduk copper mine, Iran, using CART, MVRA (multivariate regression analysis) and different empirical models considering 86 blast events and two effective parameters (MCPD and monitoring distance). They concluded that the CART technique performed best ($R^2 = 0.95$ and RMSE 0.17) and can generalise results. Similarly, Khandelwal et al. [6] estimated PPV of an open cast coal mine of Singareni Collieries Company Limited, Telangana, India, using CART, MVRA and empirical models. They concluded that the performance of CART in predicting PPV was superior to other examined models. In both studies, only two parameters (MCPD and monitoring distance) were considered for predicting PPV.

Amongst all the soft computing techniques, the applicability of ANN has been widely investigated. Hence, the present study compares the results obtained from the CART model with the ANN model. Similar to the human brain, ANN also

consists of a massively interconnected network of neurons for parallel and non-linear information transfer [7]. ANN is initially trained by some known examples of a problem to acquire knowledge. Once the ANN is trained, the network is capable of predicting the unspecified instances of the problem. ANN is well accepted amongst scientists and researchers as an important tool for solving a complex problem and real-world applications. In the field of rock mechanics and tunnelling technology, researchers have widely applied ANN to predict laboratory results [8, 9]. The past researchers have established that ANN is a versatile tool which can effectively predict fly-rock, back-break, over-break and ground vibrations in mines. In an interesting study, Amnieh et al. [10] applied ANN in Sarcheshmeh opencast copper mine, for predicting burden, spacing and total weight of explosives using PPV and other parameters such as block volume and explosive type as input. Monjezi et al. [11] implemented ANN to predict fly-rock in blasting using nine input parameters at Sungun opencast mine. The study concluded that ANN is superior to Lundborg and other statistical models. Mohamed [12] predicted blast vibrations of a limestone quarry in Egypt using ANN. He also investigated the effect of a different number of input variables on ANN for predicting ground vibrations. In their model, MCPD, distance from the blasting face to the monitoring point, stemming and hole depths were taken as input parameters to predict PPV. It was concluded that the prediction results obtained from different models of ANN are more reliable than those obtained from the tradition scaling laws. Furthermore, they established that the PPV is highly affected by the parameter 'distance from the blasting face' and is least affected by the parameter 'stemming'. Similarly, Alvarez-Vigil et al. [13] found that blast-induced PPV and frequencies at Bahoto quarry, Spain, can be effectively predicted by ANN than conventional statistics. Zhongya and Xiaoguang [14] used two intelligence science techniques, i.e. general regression neural network and support vector machine for predicting the blast-induced vibrations at Masjed-Soleiman dam, Iran. Maximum charge per delay and distance between the blast face to the monitoring point were considered as input parameters for both techniques. Results obtained from the general regression neural network and support vector machine demonstrated better correlation in comparison to empirical methods for predicting PPV. Mohamadnejad et al. [15] predicted blast-induced ground vibrations of the Gol-E-Gohar opencast iron mine, Iran, using a four-layer feed-forward back propagation model incorporating multi-layer perceptron trained with the Levenberg–Marquardt algorithm. Their ANN model was formulated using the maximum charge per delay, distance from the blasting face to the monitoring point, stemming hole depths as inputs and PPV as output. The obtained results were compared with the commonly used vibration predictor equations. They concluded that the PPV predicted by ANN is more reliable than predicted by vibration

predictor equations. Saadat et al. [16] predicted the blast-induced ground vibrations using ANN in the Siahisheh tunnelling project, Iran, and concluded that ANN is more accurate in comparison to conventional statistics and empirical methods. Moreover, Lapcevic et al. [17] studied ground vibrations at an underground copper mine in Serbia and obtained good prediction using ANN in comparison to other conventional methods.

2 Research Significance

Recent researches indicate that soft computing tools are more accurate and efficient in predicting ground vibrations. In previous attempts, Hasanipanah et al. [5] and Khandelwal et al. [6] developed decision trees for predicting vibrations using only two controllable parameters, i.e. MCPD and monitoring distance from blasting patch. However, blast-induced ground vibrations are affected by many controllable and uncontrollable parameters. Controllable parameters include geometrical parameters (hole depth, hole diameter, no. of holes, area of tunnel cross-section) and explosive-dependent parameters (explosive type, total charge, MCPD, charge per hole, etc.). Uncontrollable parameters comprise delay-time scatter, geology, rock properties, etc. The main difference between previous investigations and the present work is that in addition to the two controllable parameters considered by Hasanipanah et al. [5] and Khandelwal et al. [6], this study further considers other effective controllable parameters (total charge, tunnel cross-section, number of holes, hole diameter, hole depth, charge per hole, etc.) for developing a decision tree. The classification obtained from the decision tree using a high number of inputs may facilitate easy comprehension and control of blast vibrations on sites. Furthermore, in the previous investigations, the decision tree was developed for vibration prediction of open cast mines. In the present study, the decision tree is developed for predicting vibrations during underground excavations. The suitability of the decision tree was determined by comparing it with widely researched ANN, MVRA and other empirical models.

3 Site Description

The dataset for the investigation was compiled from observations noted at six different Indian tunnel sites. Five of the sites are situated in the Himalayas, whereas one site is located in the Aravalli mountain range. The distances between the blasting faces and monitoring stations at all sites were precisely measured using a portable GPS (global positioning system). PPV was measured using portable seismographs manufactured by Instantel. The dynamic range of the seismographs used is greater than 96 dB with frequency ranging between 2 and

250 Hz and sampling rate of 300 samples/s. Seismographs generate variation graphs of PPV and dominant frequency as outputs. The trigger levels of the seismographs used can be varied between 0.1 and 255 mm/s. Geophone of the seismograph is capable of measuring particle velocities in three orthogonal directions. A brief description of the project sites is presented below.

3.1 Chuzachen Hydro-Electric Project, East Sikkim, India

The Chuzachen Hydro-Electric Project is run-of-the-river project situated 21 km east of Rangpo City. Its power generation capacity is 110 MW. The project is built across the Rangpo and Rangoli rivers in the state of Sikkim, India. The investigation was conducted in the head race tunnel of the project. The lithology along the tunnel alignment comprises mainly of schist, gneiss, mylonite, quartzite and phyllite rocks with cross-cutting pegmatite veins. The rock mass was classified as class IV using rock mass quality (Q -system). The uniaxial compressive strength of encountered rock mass varied between 77 and 55 MPa. The cross-section of the investigated tunnel was 25 m². A double-split burn-cut pattern containing nine cut holes was used for initial cut formation. The pattern initiates with a central hole and extends using subsequent firing of holes located at the edges. Eventually, 22 breakages and 24 periphery holes were sequentially fired in the round as shown in Fig. 1a.

3.2 Karchham-Wangatoo Hydro-Electric Project, Himachal Pradesh, India

The Karchham-Wangatoo Hydro-Electric Project has a 1000-MW capacity, a run-of-the-river project built across the Sutlej River in Kinnaur district, Himachal Pradesh, India. Blasting was performed and monitored in four different excavations, namely, adit to diversion tunnel, diversion tunnel, inlet adit and main access tunnel. The rock types, tunnel cross-sectional area, rock mass classes and the blast pattern used for excavation of underground structures are shown in Table 1. The uniaxial compressive strengths of rock mass in adit to diversion, diversion tunnel, inlet adit and main access tunnel were between 115 and 64, 122–76, 95–55 and 110–75 MPa, respectively. The drilling and firing patterns used for excavating different underground structures are depicted in Fig. 1b to e.

3.3 Shongtong-Karchham Hydro-Electric Project, Himachal Pradesh, India

The Shongtong-Karchham Hydro-Electric Project is a run-of-the-river project constructed over the Sutlej River in Kinnaur district, Himachal Pradesh, India. The project is having a

capacity of generating 450 MW power. The project area and its surroundings expose one of the oldest stacks of rocks in the core Himalayas. The study was conducted in adit and diversion tunnels of the project. The metamorphic phase in the tunnels was characterised as green-schist to amphibolite facies. Rock mass classification of the tunnel as per the Q -system was 23 and designated as class II rock mass. The uniaxial compressive strength of the rock mass present in the investigated structures varied between 145 and 72 MPa. The wedge-cut pattern as shown with 11 cut, 40 breakage and 36 perimeter holes (Fig. 1f) was used for excavation.

3.4 Sawra-Kuddu Hydro-Electric Project, Himachal Pradesh, India

The Sawra-Kuddu Hydro-Electric Project is run-of-the-river scheme constructed over the Pabbar River, Himachal Pradesh to generate 111 MW power. The lithology of the area mainly comprises of quartz phyllite schist. The study was conducted in adit to head race tunnel of the project. The rock mass was moderate to highly jointed, thinly foliated and sheared. The joints were smooth and rough planar with clay-filled discontinuities. The rock mass was characterised as extremely poor to very poor category. The uniaxial compressive strength of the rock mass in the adit varied between 80 and 50 MPa. The cross-section of the tunnel was 29 m². A wedge-cut pattern with 7 cut, 14 breakage and 26 perimeter holes as shown in Fig. 1g was used for rock excavation.

3.5 Baga Transportation Tunnel, Solan, Himachal Pradesh, India

The Baga tunnel is a roadway tunnel located in Solan district of Himachal Pradesh, India. The rock type encountered along the tunnel comprises of highly fractured and weathered quartzite. The tunnel was excavated from both sides, and rock mass classified as type V was encountered throughout the alignment. The uniaxial compressive strength of rock mass varied between 52 and 42 MPa. The cross-section of the tunnel was 60 m². A pilot tunnel (5 × 2.9 m) was firstly excavated with the wedge-cut pattern. The firing sequence and blast pattern implemented for tunnel excavation are depicted in Fig. 1h.

3.6 Ghat ki Guni, Jaipur, Rajasthan

Ghat ki Guni is a twin transportation tunnel constructed at Jhalana hills in the Aravalli mountain ranges, Jaipur, Rajasthan. The area is mainly composed of Alwar and Ajabgarh rock groups consisting of calc-silicates, quartzite, grits and schistose rocks. The cross-sectional area of the tunnel was 81.2 m². The uniaxial compressive strength of the rock mass varied between 112 and 65 MPa. The tunnel was

excavated using heading (5.7 m high) and benching (2.5 m deep) with a wedge-cut pattern as shown in Fig. 1i.

Cartridge emulsion explosives as specified in Table 2 were used at the investigated sites. In India, the emulsion explosives with a diameter less than 50 mm are detonator sensitive and do not require booster for initiation. A non-electric detonating system was used in conjunction with electric blasting cap no. 8 to detonate the blast.

4 The Dataset

The compiled database consists of 137 data points monitored at different sensitive and strategic locations of the investigated sites. Generally, more than 100 data points must be considered in a dataset for obtaining reliable results using numerical models [17]. The dataset was divided in 80:20 ratio for training and testing, respectively. The parameters considered for formulating ANN, CART and MVRA models were tunnel cross-section, number of holes, hole diameter, average hole depths, average charge per hole, maximum charge per delay, total charge, powder factor and distance from the blasting face to the monitoring point. Only those parameters which can be directly controlled by the blaster were used for developing models. The statistical description of blast data is presented in Table 3. For the identification of influencing parameters, a correlation matrix was formed and is shown in Table 4. The bivariate correlation technique was used to analyse the strength of the linear relationship between the input and output parameters. The matrix helped in determining the relative influence of each input parameter on the output parameter. It can be observed from the matrix that the most and the least influencing parameters are ‘monitoring distance’ and ‘number of holes’, respectively. After compilation of the dataset, the predictive models for the PPV were formulated using conventional scaled distance laws, MVRA, ANN and CART.

5 Prediction of Blast Vibrations by Conventional Predictor Equations and MVRA

5.1 Conventional Predictor Equations

Scaled distance laws minimise the damage potential of blast vibrations by predicting PPVs against scaled distances. The prediction enables engineers to adjust MCPD to limit PPV within the safety standards. These equations generally assume that the energy of the ground motion produced by blast varies with the mass of explosives detonated per delay and monitoring distance. Various ground vibrations predictor equations

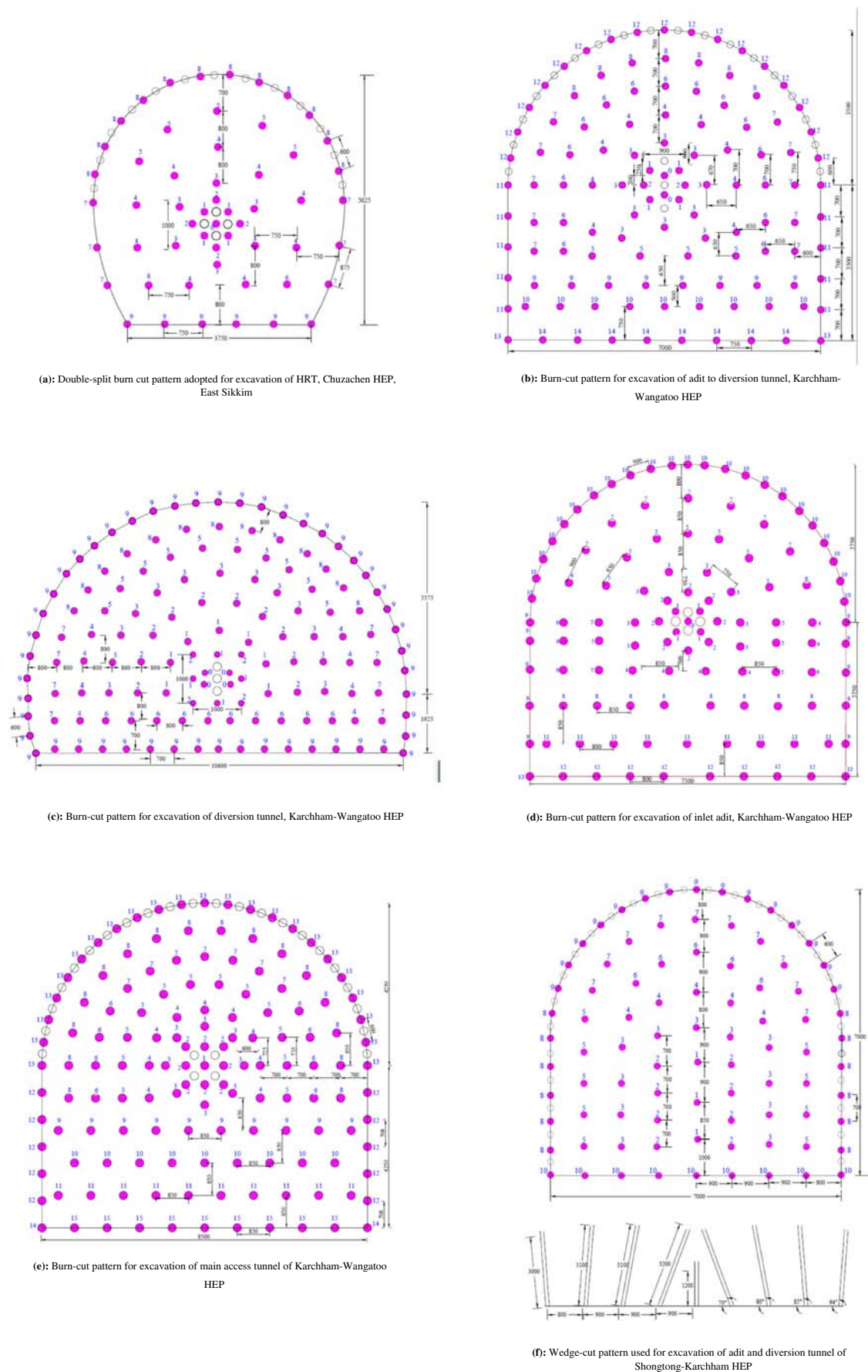
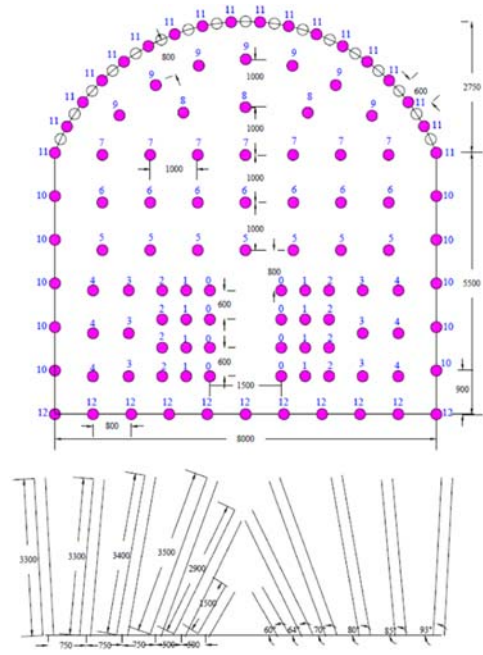
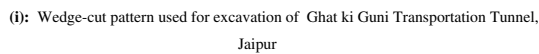


Fig. 1 Blast designs adopted at the investigated sites



(h): Wedge cut pattern for excavation of transportation tunnel, Solan, Himachal Pradesh






-  Charged hole of 45 mm diameter
-  Dummy hole of 45 mm diameter
-  Relief hole of 89 mm diameter

Fig. 1 (continued)

Table 1 Salient features of tunnels excavated at Karchham-Wangatoo Hydro-Electric Project

Structure	Rock type	Tunnel cross-section (m ²)	Rock mass class	Type of blast pattern	Blast holes type	No. of holes
Adit to diversion tunnel	Jointed augen gneiss and micaceous gneiss	43.74	III–IV	Burn cut	Cut hole	16
					Breakage hole	64
					Perimeter hole	37
Diversion tunnel	Blocky augen and micaceous gneiss	86.63	III	Burn cut	Cut hole	12
					Breakage hole	68
					Perimeter hole	50
Inlet adit	Granitic gneiss with biotite schist bands and amphibolite at few locations	50	IV	Burn cut	Cut hole	13
					Breakage hole	53
					Perimeter hole	43
Main access tunnel	Granitic gneiss with subordinate biotite schist bands at places	64.5	III	Burn cut	Cut hole	23
					Breakage hole	81
					Perimeter hole	44

Table 2 Specifications of explosives used at the investigated sites

Project	Explosive product	Manufacturer	Diameter (mm)	Weight (g)	VoD (mm/s)	Density (g/cc)
Chuzachen	Ideal power 80	Ideal	40	395	4000 ± 200	1.10–1.20
Baga tunnel, Solan	Ideal power 80	Ideal	32	185	4000 ± 200	1.10–1.20
Karchham-Wangatoo	Ideal power 90	Ideal	40	395	4500 ± 250	1.20–1.25
Karchham-Wangatoo	Ideal power 90	Ideal	40	395	4500 ± 250	1.20–1.25
Shongrong-Karchham	Super power 90	Solar	40	390	4500 ± 250	1.15–1.25
Sawra-Kuddu	Super power 80	Solar	40	390	4000 ± 200	1.25–1.25
Ghat Ki Guni tunnel	Powergel	Orica	40	390	4000 ± 200	1.07–1.25

proposed by different researchers and used in the present study are shown in Table 5. The scaled distance and PPV are plotted on log-log plane to evaluate the parameters associated with these equations. Since this is done individually for each site, the separate prediction equation was formulated for each site with individual site constant. The site constants calculated for different predictor equations are presented in Table 6. The output predicted by these predictor equations was compared with the recorded PPVs for error calculation. Two error functions, namely, RMSE and coefficient of determination (R^2), were used to check the accuracy of all the models. The relative comparison of various predictor equations is shown in Fig. 2. It can be observed that the best predictor equation for all sites was the United States Bureau of Mines.

5.2 MVRA

The relationship between a dependent variable and one or more independent variables can be modelled using MVRA. This method is an advanced version of simple linear regression and is based on the minimisation of error differences between the predicted and measured output values. The MVRA-based model has also been developed in the study for the PPV prediction. A typical MVRA model is shown in the equation

$$Y = \alpha_0 + \alpha_1 X_1 + \dots + \alpha_i X_i + e \quad (1)$$

where

Y is the predicted variable,
 X_i ($i = 1, 2 \dots n$) is the input parameters,
 α_0 is the intercept (coordinate at the origin),
 α_i ($i = 1, 2 \dots n$) is the coefficient of the i^{th} input parameter,

and e is the error associated with prediction.

A variable having significance predicted value greater than 15% is generally discarded for predicting the output. As the observed predicted values for the cross-section, no. of holes, hole diameter, hole depth, and MCPD were greater than 15%, so these parameters were neglected for formulating MVRA. The following equation has been obtained for predicting PPV using MVRA:

$$\text{PPV (mm/s)} = 31.42 - 7.24[\text{CPH, kg}] + 0.02[\text{TC, kg}] - 0.10[D, m]$$

The relation between predicted and measured PPV obtained for test data using MVRA on 1:1 slope line is shown in Fig. 3. The CoD and RMSE for MVRA equations are 0.33 and 5.93, respectively.

Table 3 Input and output parameters along with their range used for developing ANN and CART models

Project	Total charge (kg)		Tunnel cross-section (m ²)		MCPD (kg)		No. of holes		Hole diameter (m)		Monitoring distance from blast face (m)		Hole depth (m)		Average charge per hole (kg)		Observed PPV (mm/s)	
	Min	Max	Min	Max	Min	Max	Min	Max	Min	Max	Min	Max	Min	Max	Min	Max	Min	Max
Chuzachen	125	175	23.56	25.08	51.45	64.25	60	68	45	45	100	220	3	3	1.84	2.87	0.447	3.8
Baga transportation tunnel	16.5	29.25	15	15	2.2	6	30	52	45	45	12	22	1.5	3	0.55	0.76	25.7	73.2
Karchham-Wangtoo	95	575	43.74	87.61	23.51	124.3	50	245	45	45	26	300	3.9	3.9	1.022	3.97	1.02	19.5
Shongtong-Karchham	98.6	262.13	62.96	62.96	39.78	56	67	106	45	45	31	166	3	3	1.4	2.47	0.879	35.9
Sawra-Kuddu	29.25	95	29	29	4.68	25.74	25	47	34	34	60	105	1.5	1.5	1.17	2.74	0.648	7.823
Ghat ki Gunni transportation tunnel	47.4	157	54.67	54.67	15	35	63	164	32	32	9.5	24.3	2	2	0.5	1.61	8.63	71.8

Table 4 Correlation matrix with significance levels for different parameters

	Cross-section	No. of holes	Hole diameter	Hole depth	Charge/hole	MCPD	Total charge	Distance	PPV
Cross-section	1								
No. of holes	0.67	1							
Hole diameter	0.30	0.34	1						
Hole depth	0.48	0.54	0.85	1					
Charge per hole	0.35	0.18	0.52	0.65	1				
MCPD	0.58	0.64	0.54	0.63	0.53	1			
Total charge	0.71	0.74	0.59	0.74	0.75	0.78	1		
Distance	0.35	0.17	0.44	0.45	0.47	0.27	0.40	1	
PPV	-0.15	-0.07	-0.44	-0.47	-0.53	-0.23	-0.34	-0.59	1

6 Soft Computing Tools

6.1 ANN

ANN consists of multiple layers, and each layer comprises a fixed number of neurons. The number of neurons depends upon the nature of the problem. Each neuron of the individual layer is interconnected with every neuron of consecutive layers using some weights [18]. The number of neurons in the input layer is equal to the number of inputs. Similarly, the number of neurons in the output layer depends on the number of output parameters. The number of hidden layers containing neurons depends upon the complication of the problem and is usually determined by trial and error [19]. Neurons of the input layer are connected via a hidden layer to the neurons of the output layer with some weight. The schematic representation of a single neuron j is shown in Fig. 4. The output of the neuron o_j is calculated using Eq. (2).

$$o_j = f \left(\sum_{i=1}^n (w_{ij}k_i + b_j) \right) \quad (2)$$

where w_{ij} is the weight associated with the connection from input neuron i having a magnitude of p_i , b_j is the bias

associated with neuron j and f is the activation function. The neurons are activated via activation function which is, in general, a differential non-linear function like sigmoid, linear function or step function.

The feed-forward back propagation neural network has been found most suitable for predicting results in the area of rock mechanics for function approximation [20–23]. The training process in ANN is generally carried out by adjusting the biases and weights iteratively, for minimising the error and predicting results closer to the target value. There are various back propagation algorithms such as gradient descent, gradient descent with momentum, conjugate gradient, Levenberg–Marquardt and quasi-Newton approaches, which are generally used to train the model.

6.1.1 The Architecture of the ANN Network and Data Processing

The network in the present study was architected using the neural network tool (nntool) with MATLAB software. The network consists of one input layer containing eight input neurons, one hidden layer containing 19 neurons and one output layer containing a single neuron. Overfitting was prevented by using a small number of

Table 5 Summary of commonly used PPV predictor equations

Predictor equations	Empirical models
United States Bureau of Mines (1959)	$V_{ppv} = K \left(\frac{D}{\sqrt[3]{Q_{max}}} \right)^{-B}$
Langefors and Kihlstrom (1963)	$V_{ppv} = K \left(\frac{D}{D_s} \right)^B$
General Predictor (1964)	$V_{ppv} = K D^{-B} (Q_{max})^A$
Ambraseys and Hendron (1968)	$V_{ppv} = K \left(\frac{D}{\sqrt[3]{Q_{max}}} \right)^{-B}$
Bureau of Indian Standards: 6922 (1973)	$V_{ppv} = K \left(\frac{D}{D_s} \right)^B$

Table 6 Site constants used in predictor equations of the investigated tunnel

Equation for PPV	Chuzachen project			Baga transport tunnel			Karchham-Wangatoo project			Shongtong-Karchham project			Sawra-Kuddu project			Ghat ki Gunni transportation tunnel		
	K	B	A	K	B	A	K	B	A	K	B	A	K	B	A	K	B	A
United States Bureau of Mines (1959)	12,782	3.03	–	8524	2.65	–	81.51	1.14	–	3986	2.58	–	275	–1.55	–	125.7	–1.34	–
Langefors and Kihlstrom (1963)	0.006	14.25	–	52.08	1.91	–	1.35	2.356	–	0.1	8.53	–	2.77	1.72	–	5.59	–1.34	–
General Predictor (1964)	2.63	–10.75	26.68	0.0002	4.71	–0.087	71.04	–1.34	0.81	2.71	–3.02	3.69	459,019	–3.02	0.43	77.62	–1.21	0.7.
Ambraseys and Hendron (1968)	52,937	–2.85	–	4526	–2.09	–	189.5	–1.16	–	14,970	–2.46	–	3145	–2.03	–	268.3	–1.37	–
Bureau of Indian Standards: 6922 (1973)	1133	–2.66	–	52.06	0.952	–	1.353	1.178	–	0.1	4.26	–	2.77	0.86	–	5.59	1.16	–

hidden neurons. Different sizes of the network were considered for determining the number of hidden neurons and optimising network. For the training process, the Levenberg–Marquardt back propagation algorithm with Bayesian regularisation algorithm was used (applied as TRAINBR function in MATLAB software). The Levenberg–Marquardt optimisation technique optimises weights and biases associated with the network and updates the network accordingly. Squared error and weights were used as performance indices. These indices are minimised to obtain the best combination of weights for architecting the generalised network. The mean square error (MSE) function available in the nntool box was used as default performance index for optimising algorithm. A representative flowchart for construction of the ANN model is shown in Fig. 5.

Early stopping and regularisation are the two most commonly used techniques for enhancing the generalisation of the network. An early stopping criterion was used to prevent the network generalisation. The training of the network was stopped when any one of the following criteria was achieved:

- The maximum number of epoch (set as 5000).
- Maximum time allotted, i.e. 5 s.
- Minimisation of the performance function.
- Performance gradient falls below the minimum value of 1×10^{-7} .
- mu value (scalar parameter associated with the Levenberg–Marquardt algorithm) exceeds its maximum value of 1×10^{10} .

Log sigmoid function (LOGSIG) was used for training the data. The data were scaled between 0 and 1 using Eq. (3)

$$d_{\text{normalised}} = \left(\frac{d - d_{\min}}{d_{\max} - d_{\min}} \right) \quad (3)$$

where,

d_{\max} maximum value of a data point.

d_{\min} minimum value of a data point.

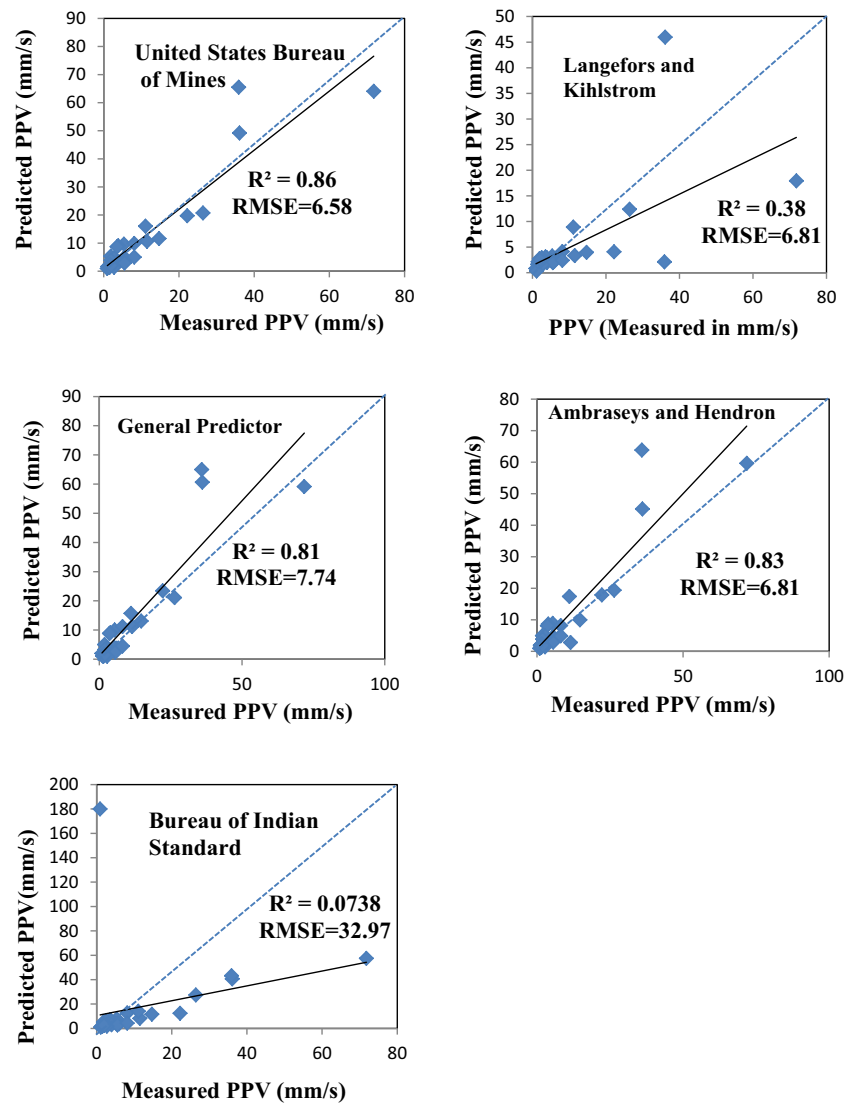
$d_{\text{normalised}}$ scaled value of a data point.

The major disadvantage of ANN is that it cannot extrapolate the dataset; hence, the testing of dataset should be examined carefully for ranging the testing dataset within the range of the training dataset.

6.1.2 Prediction of PPV Using the ANN Technique

The neural network developed for the present study contained eight input parameters and one output parameter as already presented in Table 3. Based on various trials and errors, the best result was found using 19 number of neurons in the

Fig. 2 Plots for measured vs predicted PPV by conventional predictor equations



hidden layer. The plot of mean square error vs. epoch is shown in Fig. 6. It clearly shows that the testing error does not increase above the best performing epoch depicting that the

network developed is not overlearning [24]. The measured and predicted PPV on 1:1 slope line for the ANN model is

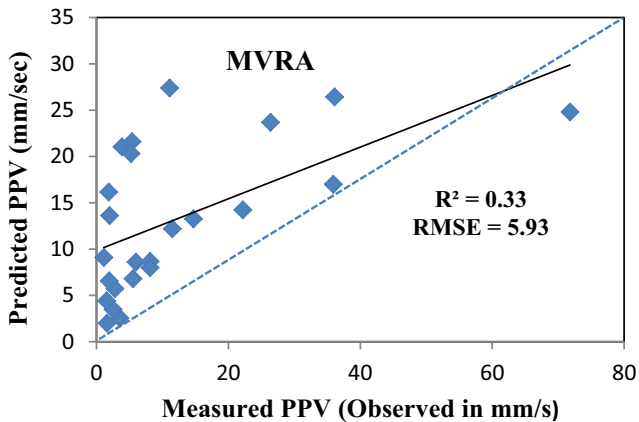


Fig. 3 Plot of measured v/s predicted PPV for MVRA

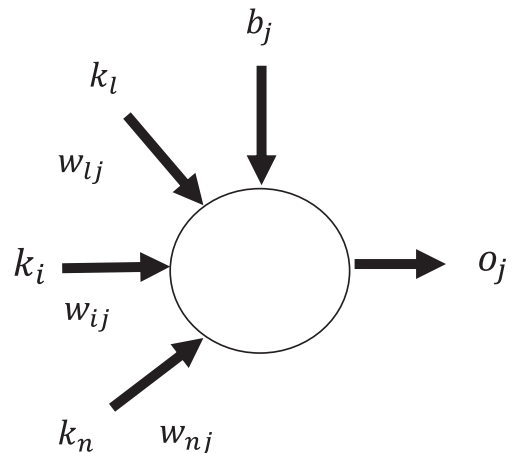


Fig. 4 The schematic representation of neuron j

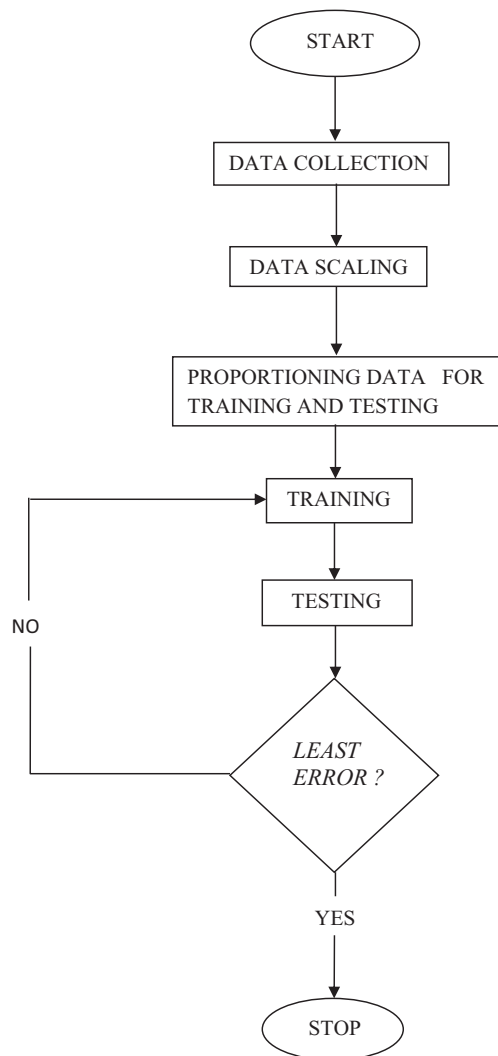


Fig. 5 A representative flowchart for construction of the ANN model

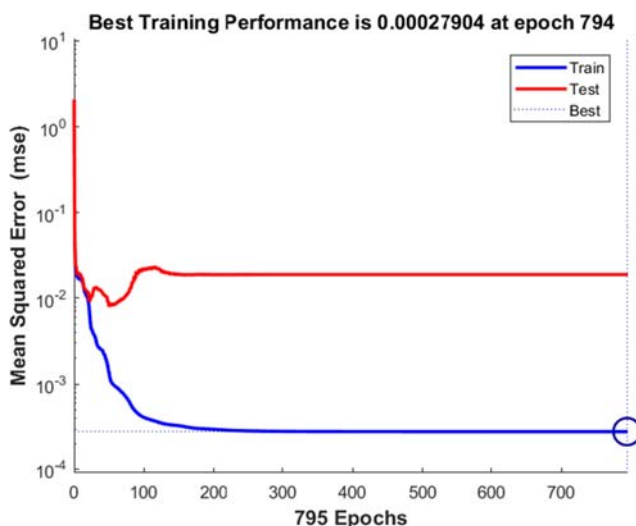


Fig. 6 Mean squared error vs epoch with best performing model

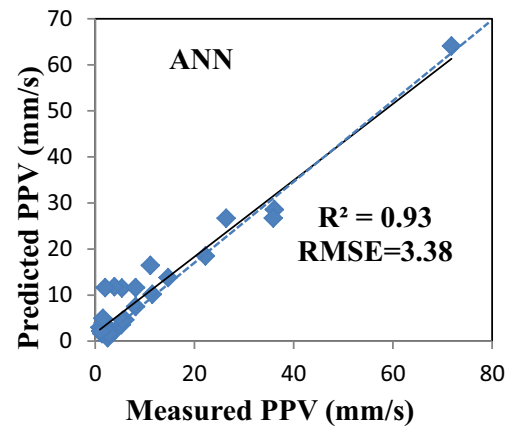


Fig. 7 Plot for measured v/s ANN predicted PPV

shown in Fig. 7. The CoD and RMSE for test data of ANN were 0.93 and 3.38, respectively.

6.2 Decision Tree and CART Technique

Classification is a general process for humans. On the other hand, numeric predictions are generally conducted using mathematical tools such as regression. However, the CART technique classifies and regresses data simultaneously using the decision tree. A decision tree is a graphical representation of results in the form of an inverted tree having roots upward and branches containing leaves at the bottom (Fig. 8). A decision tree starts with a root node (most influencing parameter) with its possible value and further branches into subsets based on homogeneity using tests. The tests compare the value with a predetermined constant for data splitting at each node. The data can be split into three or more subsets based on several if and then conditions. These processes are reiterated for each branch. The branch development is terminated using stopping criteria. An attribute is not split if all the instances at the node are classified similarly. The entire tree details about the influence of each attribute. The most influencing attribute is branched further and is termed as a root node. The target

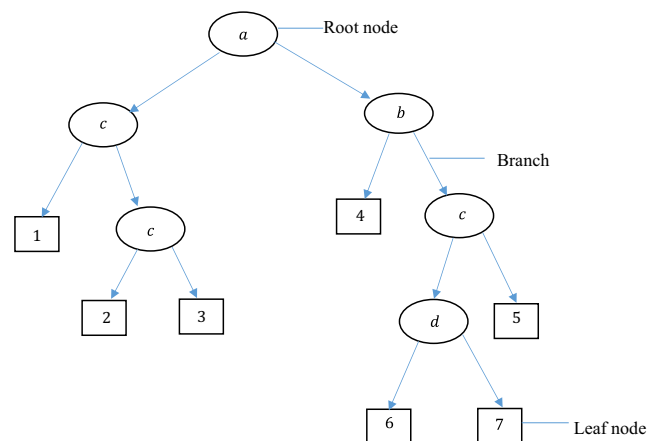


Fig. 8 Simple structure of a decision tree

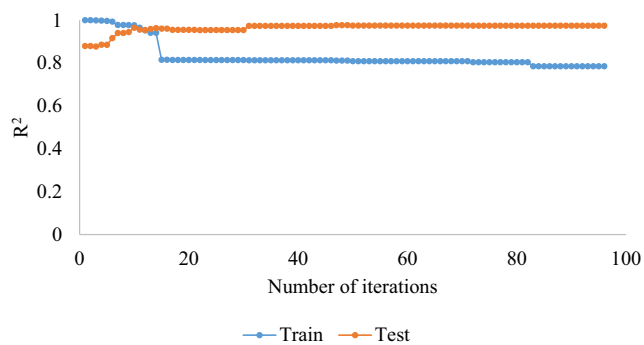


Fig. 9 Plot between R^2 and number of iterations of train and test dataset

values may be predicted using a combination of nodes or individual node.

The model was built in MATLAB software using numerical codes. Hundred iterations were performed for training the dataset. Each training iteration yielded a decision tree with CoD. At the 10th iteration, the proximate values of CoD were obtained for training and testing datasets (Fig. 9), indicating the absence of overfitting. Hence, the decision tree at the 10th iteration with $\text{CoD}_{\text{test}} = 0.95$ and $\text{RMSE}_{\text{test}} = 1.560$ was finalised for predicting PPV and classifying blast-related parameters (Fig. 10).

The decision tree obtained at the 10th iteration is depicted in Fig. 11. It suggests that PPV is primarily influenced by monitoring distance (root node of the tree). For a distance less than 11.7 m, the value of PPV is expected to be 69.75 mm/s. For monitoring distances between 11.7 and 16.25 m, the expected PPV of blasts reduces to 37.7 mm/s. Similarly, for distances between 16.25 and 39 m, total charge plays a pivotal role in predicting blast-induced vibrations. PPV at these distances can be reduced from 28.5 to 16.774 mm/s by limiting the total charge below 113 kg. The cross-section of the tunnel governs the intensity of blast-induced ground vibration for distances 39 to 59 m. However, for distances between 59 and 127.5 m, MCPD plays a pre-dominant role in controlling vibrations. Furthermore, the magnitude of PPV at these distances can be reduced by limiting MCPD below 93.485 kg;

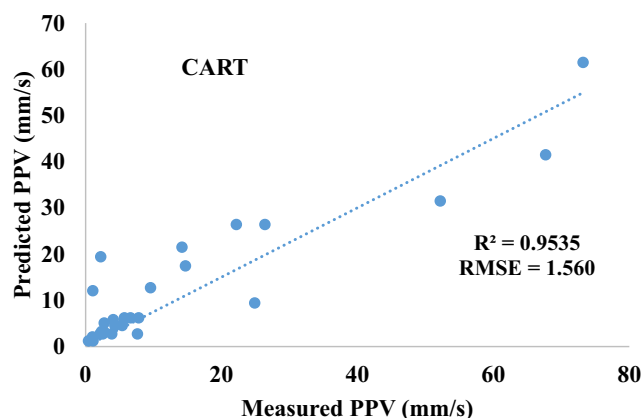


Fig. 10 Plot between PPV measured and predicted by CART

this can be easily achieved by using a greater number of delays. However, distances beyond 127.5 m are primarily influenced by charge per hole. Hence, the decision tree indicated that the near-field vibrations in underground blasting are mainly influenced by total charge fired in a complete cycle (composed of several rounds). The use of proper delay intervals can help in controlling PPV between distances 59 and 127.5 m. However, explosive charge in every hole is to be controlled for limiting far-field vibrations (beyond 127.5 m) in tunnel blasting. Hence, the rules prescribed in the decision tree can be readily used for controlling blast-induced vibrations at the investigated sites.

7 Evaluation of Models' Performance

The PPV predicted using the test data were correlated with measured PPV for performance evaluation. All the formulated models (CART, ANN, MVRA and conventional predictors) were compared to each other using performance indices. The comparison of different models is presented in Table 7. The CART model outperformed all the other models as a high CoD with low RMSE was obtained for it. The performance of the ANN model was better in comparison to MVRA, USBM and other convention predictors (Figs. 2, 3 and 7). Thus, the results indicate that the CART model developed in the present study may be used for predicting PPV at all the sites considered in the study. CART being a rule-based method can be easily implemented on sites for controlling and predicting blast-induced ground vibrations.

8 Conclusions

Precise and efficient prediction of PPV enables minimising blast-induced nuisances. The present research compares CART, ANN, MVRA and conventional empirical predictors to predict blast-induced nuisances in some Indian tunnels. This was achieved by compiling a dataset of 137 data points from six tunnelling sites. The dataset was further split in a ratio of 80:20 for developing and testing the models. The numerical models were developed using eight controllable input parameters (total charge, tunnel cross-section, maximum charge per delay, number of holes, hole diameter, distance from blasting face, hole depth and charge per hole) which can be easily regulated on-site by blast designers. The preciseness of the developed models was compared using the magnitude of two statistical functions (R^2 and RMSE). The decision tree-based CART model is superior in predicting PPV when compared to ANN, MVRA and other conventional predictors. The R^2 and RMSE for the decision tree-based model were 0.95 and 1.56, respectively. Rules prescribed in the decision tree can be easily implemented by blast designers on the sites for

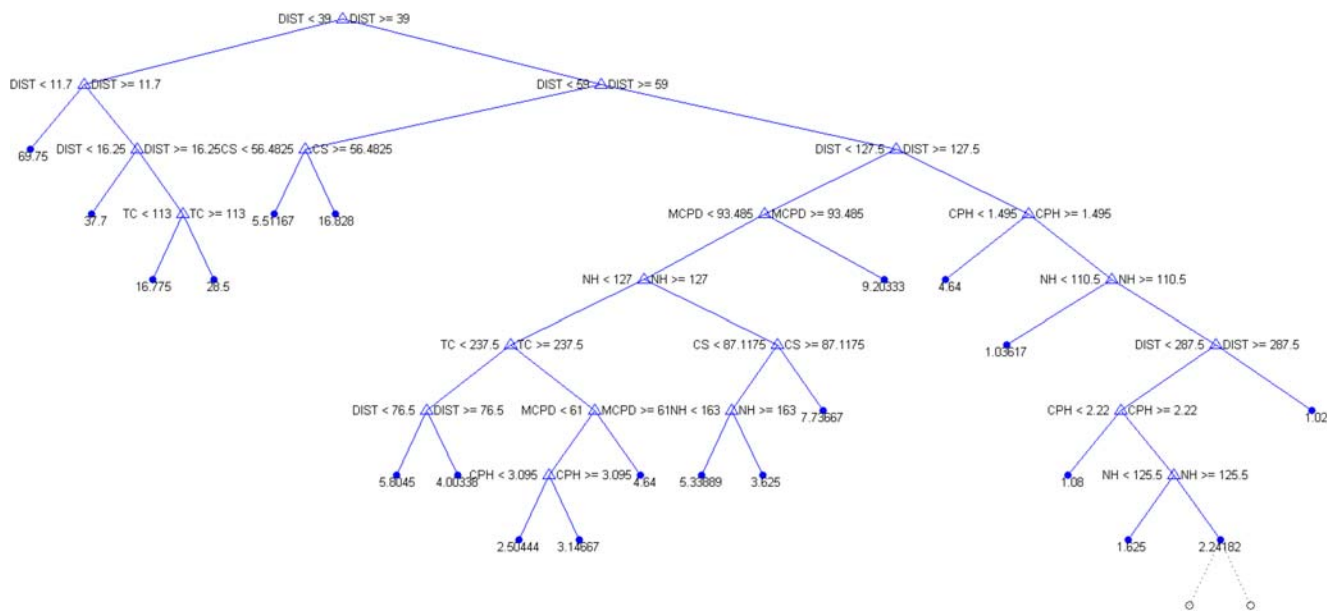


Fig. 11 Decision tree for predicting PPV (mm/s) at the investigated tunnels

controlling PPV. The decision tree indicated that near-field ground vibrations are mainly affected by total charge fired in a round. The intensity of far-field vibrations (greater than 50 m) can be controlled by adjusting MCPD and charge per hole. The results of the study indicate that the decision tree is an accurate and handy technique for limiting the vibrations on-site.

Acknowledgements The authors gratefully acknowledge the generous time and insightful comments provided by anonymous peer reviewers to enhance the quality of the paper.

Funding Information This work was supported by the Council of Scientific and Industrial Research-Central Institute of Mining and Fuel Research, India, by grant number MLP-105/18-19.

Compliance with Ethical Standards

Conflict of Interest The authors declare that they have no conflict of interest.

Table 7 Performance comparison of different models

Predictive model	Training		Testing	
	R^2	RMSE	R^2	RMSE
ANN	0.92	3.85	0.93	3.38
CART	0.97	1.05	0.95	1.56
MVRA	0.52	39.2	0.33	5.93
United States Bureau of Mines (1959)	0.87	4.30	0.86	6.58
Langefors and Kihlstrom (1963)	0.55	5.09	0.38	6.81
General Predictor (1964)	0.16	34.71	0.81	7.74
Ambraseys and Hendron (1968)	0.82	4.78	0.83	6.81
Bureau of Indian Standards 6922 (1973)	0.07	27.85	0.07	32.97

References

- Satici O, Hindistan A (2000) Drilling and blasting as a tunnel excavation method. Dissertation, Middle East Technical University.
- Monjezi M, Dehghani H (2008) Evaluation of effect of blasting pattern parameters on back break using neural networks. *Int J Rock Mech Min Sci* 45:1446–1453 <https://doi.org/10.1016/j.ijmms.2008.02.007>
- Ak H, Konuk A (2008) The effect of discontinuity frequency on ground vibrations produced from bench blasting: a case study. *Soil Dyn Earthq Eng* 28:686–694 <https://doi.org/10.1016/j.soildyn.2007.11.006>
- Khandelwal M, Singh TN (2009) Prediction of blast-induced ground vibration using artificial neural network. *Int J Rock Mech Min Sci* 46:1214–1222 <https://doi.org/10.1016/j.ijmms.2009.03.004>
- Hasanipanah M, Faradonbeh RS, Amnieh HB, Armaghani DJ, Monjezi M (2017) Forecasting blast-induced ground vibration developing a CART model. *Eng Comput* 33:307–316 <https://doi.org/10.1007/s00366-016-0475-9>
- Khandelwal M, Armaghani DJ, Faradonbeh RS, Yellishetty M, Majid MZA, Monjezi M (2017) Classification and regression tree technique in estimating peak particle velocity caused by blasting. *Eng Comput* 33:45–53 <https://doi.org/10.1007/s00366-016-0455-0>
- Khandelwal M, Singh TN (2006) Prediction of blast induced ground vibrations and frequency in opencast mine: a neural network approach. *J Sound Vib* 289:711–725 <https://doi.org/10.1016/j.jsv.2005.02.044>
- Meulenkamp F, Alvarez Grima M (1999) Application of neural networks for the prediction of the unconfined compressive strength (UCS) from Equotip hardness. *Int J Rock Mech Min Sci* 36:29–39 [https://doi.org/10.1016/S0148-9062\(98\)00173-9](https://doi.org/10.1016/S0148-9062(98)00173-9)
- Rukhaiyar S, Samadhiya NK (2017) A polyaxial strength model for intact sandstone based on artificial neural network. *Int J Rock Mech Min Sci* 95:26–47 <https://doi.org/10.1016/j.ijmms.2017.03.012>
- Bakhshandeh Amnieh H, Siamaki A, Soltani S (2012) Design of blasting pattern in proportion to the peak particle velocity (PPV): artificial neural networks approach. *Saf Sci* 50:1913–1916 <https://doi.org/10.1016/j.ssci.2012.05.008>

11. Monjezi M, Mehrdaneh A, Malek A, Khandelwal M (2013) Evaluation of effect of blast design parameters on flyrock using artificial neural networks. *Neural Comput Applic* 23:349–356 <https://doi.org/10.1007/s00521-012-0917-2>
12. Mohamed MT (2009) Artificial neural network for prediction and control of blasting vibrations in Assiut (Egypt) limestone quarry. *Int J Rock Mech Min Sci* 46:426–431 <https://doi.org/10.1016/j.ijrmms.2008.06.004>
13. Alvarez-Vigil AE, Gonzalez-Nicieza C, Lopez Gayarre F, Alvarez-Fernandez MI (2012) Predicting blasting propagation velocity and vibration frequency using artificial neural networks. *Int J Rock Mech Min Sci* 55:108–116 <https://doi.org/10.1016/j.ijrmms.2012.05.002>
14. Zhongya Z, Xiaoguang J (2018) Prediction of peak velocity of blasting vibration based on artificial neural network optimized by dimensionality reduction of FA-MIV. *Math Probl Eng*. <https://doi.org/10.1155/2018/8473547>
15. Mohamadnejad M, Gholami R, Ataei M (2012) Comparison of intelligence science techniques and empirical methods for prediction of blasting vibrations. *Tunn Undergr Sp Technol* 28:238–244. <https://doi.org/10.1016/j.tust.2011.12.001>
16. Saadat M, Khandelwal M, Monjezi M (2014) An ANN-based approach to predict blast-induced ground vibration of Gol-E-Gohar iron ore mine, Iran. *J Rock Mech Geotech Eng* 6:67–76. <https://doi.org/10.1016/j.jrmge.2013.11.001>
17. Lapcevic R, Kostic S, Pantovic R, Vasovic N (2014) Prediction of blast-induced ground motion in a copper mine. *Int J Rock Mech Min Sci* 69:19–25. <https://doi.org/10.1016/j.ijrmms.2014.03.002>
18. Atkinson PM, Tatnall ARL (1997) Introduction: neural networks in remote sensing. *Int J Remote Sens* 18:699–709. <https://doi.org/10.1080/014311697218700>
19. Kanungo DP, Arora MK, Sarkar S, Gupta RP (2006) A comparative study of conventional, ANN black box, fuzzy and combined neural and fuzzy weighting procedures for landslide susceptibility zonation in Darjeeling Himalayas. *Eng Geol* 85:347–366. <https://doi.org/10.1016/j.enggeo.2006.03.004>
20. Rafiai H, Jafari A, Mahmoudi A (2013) Application of ANN-based failure criteria to rocks under polyaxial stress conditions. *Int J Rock Mech Min Sci* 59:42–49. <https://doi.org/10.1016/j.ijrmms.2012.12.003>
21. Maji VB, Sitharam TG (2008) Prediction of elastic modulus of jointed rock mass using artificial neural networks. *Geotech Geol Eng* 26:443–452. <https://doi.org/10.1007/s10706-008-9180-9>
22. Ocak I, Seker SE (2012) Estimation of elastic modulus of intact rocks by artificial neural network. *Rock Mech Rock Eng* 45: 1047–1054. <https://doi.org/10.1007/s00603-012-0236-z>
23. Rafiai H, Jafari A (2011) Artificial neural networks as a basis for new generation of rock failure criteria. *Int J Rock Mech Min Sci* 48: 1153–1159. <https://doi.org/10.1016/j.ijrmms.2011.06.001>
24. Rukhaiyar S, Samadhiya NK (2017) A polyaxial strength model for intact sandstone based on artificial neural network. *Int J Rock Mech Min Sci* 95:26–47. <https://doi.org/10.1016/j.ijrmms.2017.03.012>

Publisher's Note Springer Nature remains neutral with regard to jurisdictional claims in published maps and institutional affiliations.